

Mechanistic Analysis of Ion Association between Dendrigrraft Poly- l -lysine and 8-Anilino-1-naphthalenesulfonate at Liquid|Liquid Interfaces

メタデータ	言語: eng 出版者: 公開日: 2018-04-05 キーワード (Ja): キーワード (En): 作成者: メールアドレス: 所属:
URL	https://doi.org/10.24517/00050466

This work is licensed under a Creative Commons Attribution-NonCommercial-ShareAlike 3.0 International License.



Mechanistic Analysis of Ion Association between Dendrigrraft Poly-L-lysine and 8-Anilino-1- naphthalenesulfonate at Liquid|Liquid Interfaces

Hirohisa Nagatani^{,†}, Masataka Fujisawa[‡], and Hisanori Imura[†]*

[†] Faculty of Chemistry, Institute of Science and Engineering, Kanazawa University, Kakuma,
Kanazawa 920-1192, Japan

[‡] Division of Material Chemistry, Graduate School of Natural Science and Technology,
Kanazawa University, Kakuma, Kanazawa 920-1192, Japan

*To whom correspondence should be addressed: H. Nagatani

E-mail: nagatani@se.kanazawa-u.ac.jp

ABSTRACT

Molecular association between biocompatible dendritic polymers, dendrigraft poly-L-lysines (DGLs), and an anionic fluorescent probe, 8-anilino-1-naphthalenesulfonate (ANS^-), was studied at the polarized water|1,2-dichloroethane (DCE) interface. The fluorescence intensity of ANS measured in aqueous solution was enhanced by the coexistence of DGL over a wide pH range ($2 < \text{pH} < 10$), where ANS and DGL exist as a monoanionic form and polycation, respectively. The voltammetric responses indicated that the positively charged DGL was adsorbed at the water|DCE interface, while ANS^- was transferred across the interface accompanied by the adsorption process. The interfacial behavior of the DGL-ANS associates was analyzed by potential-modulated fluorescence (PMF) spectroscopy. The PMF results demonstrated that the ion association between DGLs and ANS at the water|DCE interface is strongly affected by the applied potential and the dendritic generation of DGL. By applying appropriate potentials, the ANS anion was dissociated from its ion associate with DGLs at the interface and transferred into the organic phase, whereas DGLs remained in the aqueous phase. The Gibbs free energy of ion association ($\Delta G_{\text{D}\dots\text{ANS}}$) was estimated for the second-fourth generation DGLs (DGL-G2-G4) and the G4 polyamidoamine (PAMAM) dendrimer as a control. The highest stability of the DGL-G4-ANS associate manifested itself through $\Delta G_{\text{D}\dots\text{ANS}}$: DGL-G4-ANS ($>$ G4 PAMAM dendrimer-ANS) $>$ DGL-G3-ANS $>$ DGL-G2-ANS. The results elucidated the efficient anion-binding ability of higher generation DGLs and its potential-dependence at the liquid|liquid interface.

Keywords: Dendrigraft poly-L-lysine (DGL); polyamidoamine (PAMAM) dendrimer; interface between two immiscible electrolyte solutions (ITIES); potential-modulated fluorescence (PMF) spectroscopy; ion association

1. INTRODUCTION

Various organic materials including polymers and self-assembled molecular architectures based on amphiphilic molecules (micelles, vesicles, liposomes etc.) have been studied as molecular containers (carriers) and functional platforms for the drug or gene delivery to cells and tissue.¹⁻³ The polymer materials are especially useful to acquire desirable properties for their application. The physicochemical properties of polymer material depend significantly on the polymerization degree which is not strictly controllable in the case of conventional linear and cross-linking polymers. Dendritic polymers are nontraditional polymer materials with three dimensional hierarchical molecular architecture.⁴⁻⁶ The interior cavity of dendritic polymers are functional for stable encapsulation of a variety of small molecules. The molecular size of the dendritic polymers basically increases with increasing dendritic generation, i.e., degree of branching. The dendrimers have well-defined molecular structures consisting of core, interior and periphery moieties with extremely narrow molecular weight distribution, whereas the hyperbranched polymers have relatively polydisperse frameworks. The dendrigraft polymers have intermediate structural properties among the dendritic polymers. Dendrigraft poly-L-lysine (DGL) composed of amino acid lysines as a repeat unit is a water-soluble polycation with biocompatibility and biodegradability.⁷ Actually, the linear poly-L-lysine (PLL) is commonly used for surface coating to attach biomaterials such as proteins and living cells on solid surfaces through electrostatic interaction. The higher generation DGLs are roughly spherical molecules and positively charged under physiological conditions.^{8, 9} The membrane translocation properties of DGL and its guanidinylated derivatives have been studied on liposomal and cellular membranes by Theodossiou and his coworkers, reporting that DGLs efficiently localize in the nucleus and nuclear

membrane.¹⁰ DGLs are thus potential candidates for molecular carrier in drug or gene delivery applications.¹¹⁻¹⁵

Electrochemistry at the interface between two immiscible aqueous and organic solutions enables us to determine physicochemical parameters of ionizable species such as the Gibbs energy of transfer and the partition coefficient.¹⁶ The liquid|liquid interface is a simple model of biomembrane surfaces, where the pharmacokinetic mechanism of physiologically active substances and drug molecules has been investigated.¹⁷⁻²¹ Recently, the molecular association behavior between ionic species and dendritic polymers has been studied at the water|1,2-dichloroethane (DCE) interface.²²⁻²⁵ The spectroelectrochemical analysis elucidated that the interfacial mechanism of ionic species is considerably influenced by the dendritic polymers. Widely used polyamidoamine (PAMAM) dendrimers, for instance, associate with ionic species in aqueous solution, while the association-dissociation process in the interfacial region is reversibly controlled as a function of the Galvani potential difference between the water and organic phases.^{26, 27} The mechanistic analysis of the dendritic polymer associated with guest molecules at the liquid|liquid interface is crucial to evaluate the mass transfer and transmembrane properties in biomedical applications. Although Herzog *et al.* reported fundamental voltammetric response of DGL at the water|DCE interface,^{28, 29} the molecular association behavior of biocompatible dendritic polymer has not been investigated at liquid|liquid interfaces.

In this study, the molecular association between various generations of DGL and an anionic fluorescent probe, 8-anilino-1-naphthalenesulfonate (ANS^-), was studied at the polarized water|DCE interface by potential modulated fluorescence (PMF) spectroscopy. The association behavior of the ANS anion with DGLs was strongly affected by the dendritic generation and the Galvani potential difference. The association stability between dendritic polymers and ANS was

quantitatively estimated through considerable potential shifts on the ANS transfer across the interface.

2. EXPERIMENTAL SECTION

2.1. Reagents. The second–fourth generation (G2–G4) DGLs were purchased from COLCOM (Montpellier, France). The number-average degrees of polymerization and polydispersity indices of DGLs are (G2) 48 and 1.38, (G3) 123 and 1.46, and (G4) 365 and 1.36, respectively.³⁰ The amino-terminated G4 PAMAM dendrimer with ethylenediamine core (Aldrich, 10 wt% in methanol) was also examined as a control for DGLs. 8-Anilino-1-naphthalenesulfonic acid (TCI, >95%) was used as received. The composition of the electrochemical cells is shown in **Figure 1**. The supporting electrolytes were $1.0 \times 10^{-2} \text{ mol dm}^{-3}$ LiCl for the aqueous phase and $5.0 \times 10^{-3} \text{ mol dm}^{-3}$ bis(triphenylphosphoranylidene)ammonium tetrakis(pentafluorophenyl)borate (BTPPATPFB) for the organic phase, respectively. BTPPATPFB was prepared by the metathesis of bis(triphenylphosphoranylidene)ammonium chloride (BTPPACl) (Aldrich, >97%) and lithium tetrakis(pentafluorophenyl)borate (LiTPFB) ethylether complex (TCI, $\geq 70\%$). The aqueous solutions were prepared with purified water by a Milli-Q system (Millipore, Direct-Q3UV). The purified water and 1,2-dichloroethane (DCE) of HPLC grade (Nacalai Tesque, >99.7%) were saturated with each other and used as solvents in the spectroelectrochemical measurement. All other reagents were of the highest grade available. The pH condition of the aqueous phase was adjusted by the addition of HCl, phosphate buffer ($\text{LiH}_2\text{PO}_4/\text{LiOH}$) or LiOH.



Figure 1. Composition of the electrochemical cell.

2.2. Apparatus. The spectroelectrochemical cell was analogous to one reported previously.³¹ The water|DCE interface with a geometrical area of 0.50 cm² was polarized by a four-electrode potentiostat (Hokuto Denko, HA1010mM1A). Platinum wires were used as counter electrodes in both aqueous and organic phases. The Luggin capillaries were provided for the reference electrodes (Ag/AgCl) in both phases. The Galvani potential difference ($\Delta_o^w\phi \equiv \phi^w - \phi^o$) was estimated by taking the formal transfer potential ($\Delta_o^w\phi_{\text{TMA}^+}^{\circ}$) of tetramethylammonium as 0.160 V.³² UV-vis absorption and fluorescence spectra were measured by a JASCO V-630 UV-vis spectrophotometer and a JASCO FP-8300 spectrofluorometer, respectively. All experiments were carried out in a thermostated room at 298±2 K.

2.3. Potential-Modulated Fluorescence Spectroscopy. The water|DCE interface was illuminated in total internal reflection (TIR) mode from the organic phase by a cw laser diode at 404 nm (Coherent, CUBE 405-50C). The angle of incidence of the laser beam (ψ) was ca. 75° with respect to the interface normal. The fluorescence from the interfacial region was collected perpendicularly to the interface by an optical fiber and a monochromator equipped with a photomultiplier tube (Shimadzu, SPG-120S). The ac potential modulation superimposed on the dc bias ($\Delta_o^w\phi_{\text{dc}}$) was applied to the water|DCE interface.

$$\Delta_o^w\phi = \Delta_o^w\phi_{\text{dc}} + \Delta_o^w\phi_{\text{ac}} \exp(j\omega t) \quad (1)$$

where j is an imaginary number and ω is the angular frequency. The amplitude of the ac potential modulation ($\Delta_o^w\phi_{\text{ac}}$) was 0.020 V at 1 Hz and the linear sweep rate of $\Delta_o^w\phi_{\text{dc}}$ was 0.005 mV s⁻¹ unless otherwise noted. The ac modulated fluorescence signal arising from the potential-driven interfacial process of ANS and its associates with the dendritic polymers was analyzed as a function of ac potential modulation by a digital lock-in amplifier (NF, LI5640).

3. RESULTS AND DISCUSSION

3.1. Association Behavior between DGLs and ANS in Aqueous Solution. DGLs are roughly spherical molecules with hydrodynamic radii of (DGL-G2) 1.8 nm, (DGL-G3) 3.4 nm, and (DGL-G4) 6.2 nm at pH 7.0, respectively, and their free volume fractions are reported as ~ 0.8 .³⁰ Those structural properties of DGL are suitable for incorporating small molecules. ANS is a polarity-sensitive fluorescent probe which emits intense blue-shifted fluorescence in a hydrophobic environment, such as organic solvent, biomembrane, hydrophobic binding site of proteins etc.^{33, 34} The molecular association between nonfluorescent DGLs and ANS was investigated through the fluorescence intensity and the blue-shift of emission maximum. As shown in **Figure 2a**, the fluorescence intensity of the ANS probe measured under neutral pH conditions (pH 7.0–7.2) was effectively enhanced in the presence of the equimolar DGL. In addition, the emission maximum wavelength ($\lambda_{em,max}$) showed significant blue-shifts from the intrinsic maximum of ANS at 547 nm, i.e., (DGL-G2) 540 nm, (DGL-G3) 525 nm, and (DGL-G4) 507 nm. These fluorescence enhancements reveal an efficient association of ANS with DGLs in aqueous solution. The pH dependences of the fluorescence intensity in **Figure 2b** exhibit the molecular association over a wide pH range ($2 < \text{pH} < 10$). DGL has two protonatable functional groups, i.e., α -amino group ($\text{p}K_{a1,DGL} < 7.8$) and ϵ -amino group ($\text{p}K_{a2,DGL} = 10.5$).⁹ Considering the protonation equilibria of the ϵ -amino group of lysine residue side chains, the ANS probe ($\text{p}K_{a,ANS} = 1.9 \pm 0.3$ estimated from a fluorometric titration) electrostatically interacts with DGL at $\text{p}K_{a,ANS} < \text{pH} < \text{p}K_{a2,DGL}$. It should be noted that the shortest $\lambda_{em,max}$ of ANS was measured around pH 10, e.g. 495 nm for the DGL-G4 system (Supporting Information: **Figure S1**). Under alkaline conditions, DGLs are not fully protonated because of the lower $\text{p}K_a$ value for α -amino groups and DGLs could render less polar

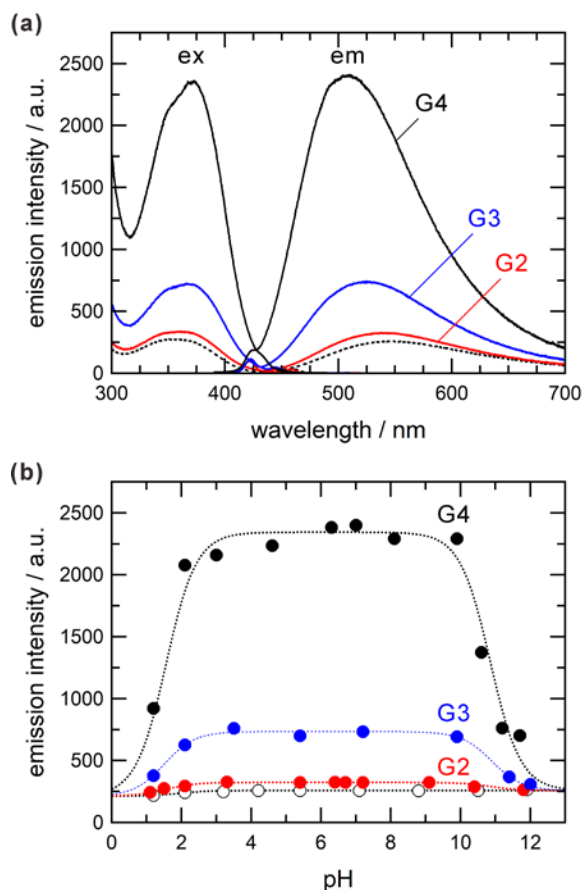


Figure 2. (a) Excitation and emission spectra of ANS in aqueous solution in the presence of equimolar DGL, and (b) pH dependences of fluorescence intensity. (a) The black, blue, and red solid lines depict the DGL-G4-ANS (pH 7.0), G3-ANS (pH 7.2), and G2-ANS (pH 7.2) systems, respectively. The dotted lines are intrinsic spectra of ANS at pH 7.0. (b) The black, blue, and red closed circles depict the DGL-G4-ANS (507 nm), G3-ANS (525 nm), and G2-ANS (540 nm) systems, respectively. The open circles refer to the fluorescence intensity of ANS at 547 nm in the absence of DGL. The excitation wavelength was 370 nm. The pH condition was adjusted by adding HCl or LiOH. The concentration of ANS and DGL was $1.0 \times 10^{-5} \text{ mol dm}^{-3}$.

binding sites for the ANS probe. The fluorescence enhancement and the blue-shift of $\lambda_{em,max}$ emphasize the stable electrostatic association of ANS anions with higher generation DGL

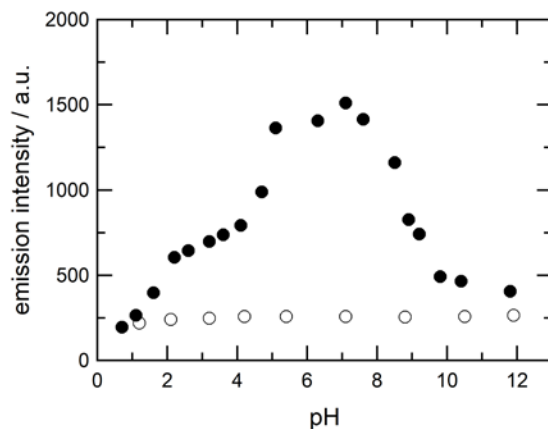


Figure 3. pH dependences of fluorescence intensity of ANS in aqueous solution in the presence and absence of equimolar G4 PAMAM dendrimer. (a) The closed and open circles depict the G4 PAMAM-ANS (513 nm) and ANS alone (547 nm) systems, respectively. The excitation wavelength was 370 nm. The pH condition was adjusted by adding HCl or LiOH. The concentration of ANS and the G4 PAMAM dendrimer was 1.0×10^{-5} mol dm⁻³.

polymers having larger positive net charges.

The electrostatic interaction of ANS⁻ with the polycationic dendritic polymer was also investigated by employing the cationic G4 PAMAM dendrimer as a control system. The G4 PAMAM dendrimer has positive charges depending on protonation equilibria of 62 tertiary amines as branch points ($pK_{a1, \text{PAMAM}} = 6.65$) in the interior moiety and 64 primary amines in the periphery moiety ($pK_{a2, \text{PAMAM}} = 9.20$).^{35, 36} The G4 PAMAM dendrimer effectively associated with ANS⁻ at $2 \leq \text{pH} \leq 9$ shown in **Figure 3** and the significant blue-shift of $\lambda_{\text{em, max}}$ was observed under neutral conditions, e.g., $\lambda_{\text{em, max}} = 513$ nm at pH 7.1 (Supporting Information: **Figure S2**). The pH dependence of the fluorescence intensity correlated with the blue-shift of $\lambda_{\text{em, max}}$ is divided into two pH ranges: (i) $5 \leq \text{pH} \leq 9$ and (ii) $2 \leq \text{pH} \leq 4$. The ANS⁻ probe could interact with the protonated periphery moiety in the neutral pH range (i) and then, additionally, with the interior of

the dendrimer in the acidic pH range (ii). In the carboxylate-terminated G3.5 PAMAM dendrimer system, the encapsulation of ANS⁻ in the positively-charged interior surrounded by the anionic periphery has been reported previously, in which the monotonic fluorescence enhancement with the blue-shift of $\lambda_{em,max}$ is maximized around pH 3.²⁶ In contrast to the PAMAM dendrimer system, the wide plateau range observed in the DGL systems (**Figure 2b**) demonstrates rather equilibrated electrostatic associations between ANS⁻ and the polycationic DGLs at $pK_{a,ANS} < pH < pK_{a2,DGL}$.

The fluorescence properties of ANS in the presence of DGL were also influenced by the ionic composition of the aqueous solution. The fluorescence enhancement through the ion association was partially prevented by adding the phosphate buffer under neutral conditions (pH 7.0–7.2). In the 1.0×10^{-5} mol dm⁻³ DGL-G3–ANS system, for instance, the fluorescence intensities were weakened down to 63% and 48%, respectively, in the presence of 1.0×10^{-3} mol dm⁻³ and 5.0×10^{-3} mol dm⁻³ phosphate buffers (Supporting Information: **Figure S3**). A relatively insufficient binding of ANS to the G5 PAMAM dendrimer has been reported in the phosphate buffered saline, i.e., 0.5–0.7 ANS molecule per unit dendrimer.³⁷ Furthermore, Cottet *et al.* reported that the conformation of the PLL coil is specifically affected by the electrostatic interaction with phosphate ions.³⁸ The capillary isotachopheresis for DGL-G1–G5 and linear PLLs demonstrated that the effective charge number of DGL decreases with increasing dendritic generation due to counterion condensation.⁸ The fluorescence quenching by phosphate buffer observed in this study thus associates with the competitive binding of ANS⁻ and excess phosphate anions to the positively charged DGL. The molecular association of ionizable species with dendritic polymers and its dependence on the phosphate concentration in solution are crucial in terms of the practical use of DDS, because the local phosphate concentration in living tissues can be a trigger for the release process of drugs encapsulated in a molecular container. Indeed, an

intracellular fluid contains a higher phosphate concentration ($> 10 \times 10^{-3} \text{ mol dm}^{-3}$) in comparison with an extracellular fluid (typically $\sim 1 \times 10^{-3} \text{ mol dm}^{-3}$). The present results suggest that the anion-binding ability of DGL responds to the phosphate concentration, and it could promote the development of functional drug carriers.³⁹

3.2. Electrochemical Responses of DGLs and ANS^- at the Water|DCE Interface. The interfacial behavior of DGLs was measured under neutral pH conditions in the absence of phosphate. **Figure 4a** shows the cyclic voltammograms (CVs) of DGLs at pH 7, where the lysine groups of DGLs can fully be protonated. The voltammetric responses arising from DGLs appeared mainly at the positive edge of the potential window. The currents measured at $\Delta_0^w \phi > 0.30 \text{ V}$ were significantly decreased with decreasing supporting electrolyte concentration to $1.0 \times 10^{-6} \text{ mol dm}^{-3}$ BTTPATPFB in DCE (Supporting Information: **Figure S4**), whereas those in the negative potential region were essentially the same. The polycationic dendritic polymers often facilitate the transfer of hydrophobic supporting electrolytes from an organic phase to an aqueous phase.^{22, 40} The voltammetric responses observed at $\Delta_0^w \phi > 0.30 \text{ V}$ are therefore attributed to the facilitated ion transfer of hydrophobic anions (TPFB^-) by DGLs at the interface. The facilitated ion transfer current showed apparent dependence on the generation of DGL: $\text{DGL-G4} > \text{DGL-G3} > \text{DGL-G2}$. The results indicate that the DGL-G4 polycation effectively interacts with TPFB^- at the interface. The ac voltammograms shown in **Figure 4b** also exhibit gradual increases of the admittance at less positive potentials ($\Delta_0^w \phi > -0.05 \text{ V}$) than that of facilitated TPFB^- transfer. Those ac voltammetric responses are indicative of the potential-driven adsorption of positively-charged DGLs at the water|DCE interface.

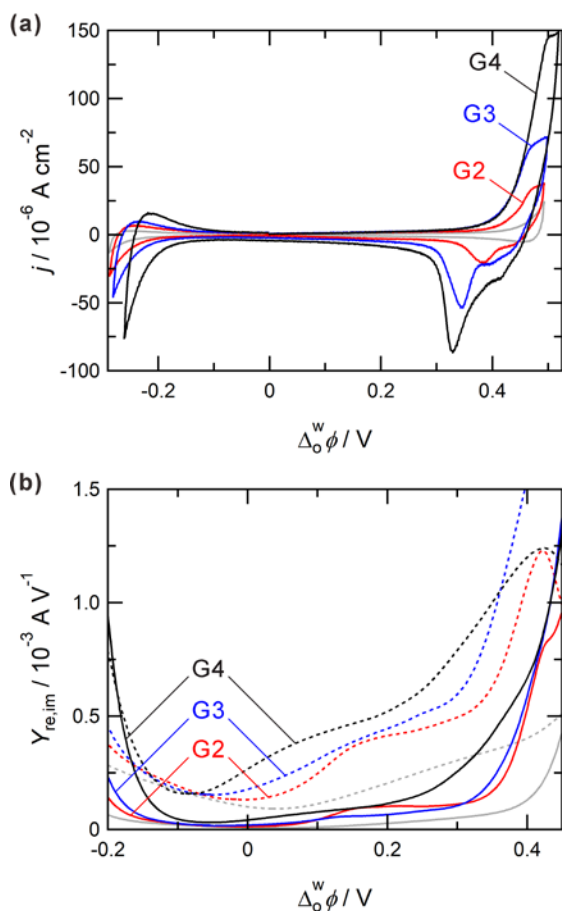


Figure 4. (a) Cyclic and (b) ac voltammograms measured for DGLs (G2–G4) at the water|DCE interface. The black, blue, and red lines depict DGL-G4 (pH 7.0), G3 (pH 7.1), and G2 (pH 7.1) systems, respectively. The gray lines were measured in the absence of DGLs. (b) The solid and dashed lines refer to the real (Y_{re}) and imaginary (Y_{im}) components of the admittance. The amplitude of ac potential modulation was 0.010 V at 7 Hz. The potential sweep rates were (a) 0.10 V s^{-1} and (b) 0.005 V s^{-1} , respectively. The concentration of DGLs was $1.0 \times 10^{-5} \text{ mol dm}^{-3}$.

The formal transfer potential of ANS^- in the absence of DGL was determined as $\Delta_0^w \phi_{\text{ANS}^-}^{\text{ot}} = -0.01 \text{ V}$ at pH 7.2, where ANS exists as a monoanionic form. The peak-to-peak separation of ca. 0.06 V and a linear relationship between the negative peak currents and the square root of

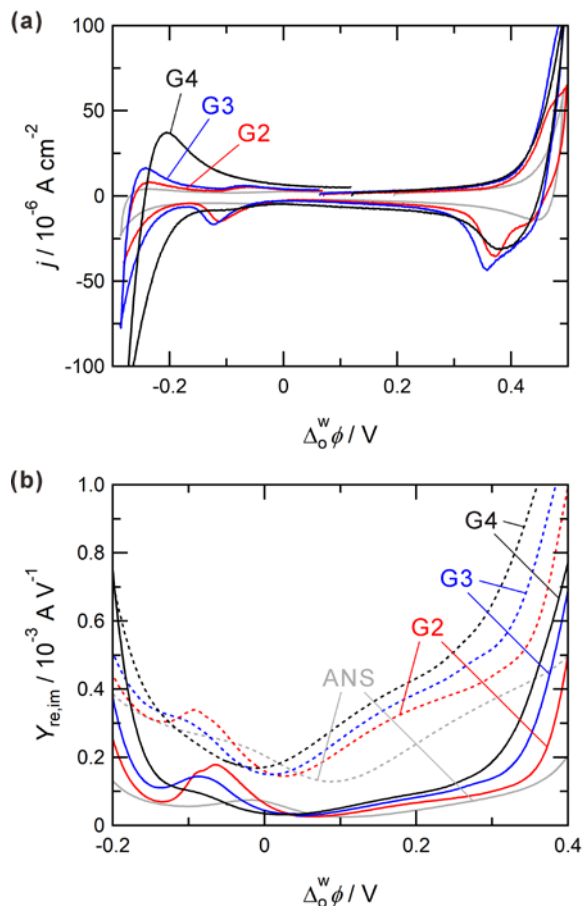


Figure 5. (a) Cyclic and (b) ac voltammograms measured in the presence of equimolar DGL and ANS. The black, blue, red, and gray lines depict the DGL-G4-ANS (pH 7.0), G3-ANS (pH 7.1), G2-ANS (pH 7.1), and ANS alone (pH 7.2) systems, respectively. (b) The solid and dashed lines refer to the real (Y_{re}) and imaginary (Y_{im}) components of the admittance. The amplitude of ac potential modulation was 0.010 V at 7 Hz. The potential sweep rates were (a) 0.10 V s^{-1} and (b) 0.005 V s^{-1} , respectively. The concentration of DGLs and ANS was $1.0 \times 10^{-5} \text{ mol dm}^{-3}$.

potential sweep rates consisted with a diffusion-controlled transfer of a monoanionic species (Supporting Information: **Figure S5**). Those fundamental electrochemical features of ANS^- are in accord with the previous report.²⁶ As shown in **Figure 5**, DGL induced significant changes in the

voltammetric response. Negative shifts of the transfer peaks of ANS^- were observed in the presence of the equimolar DGLs, in which the peak currents were linearly proportional to the potential sweep rate. The potential shift of the ANS^- transfer was relatively extended in the higher generation DGL systems: $\text{DGL-G4} > \text{DGL-G3} > \text{DGL-G2}$ (**Figure 5b**). The G4 PAMAM dendrimer was also measured as a control system and a similar negative shift in the ANS^- transfer was observed (Supporting Information: **Figure S6**). The half-wave potential of the ANS^- transfer ($\Delta_0^w \phi_{\text{ANS}}^{1/2}$) in the presence of dendritic polymers was not precisely determined from voltammetric data because of nonnegligible overlap with the adsorption response of dendritic polymers.

3.3. PMF Analysis of Molecular Association between DGLs and ANS at the Water|DCE Interface. The PMF spectroscopy allows us to analyze the interfacial process of fluorescent ions without interference from coexisting nonfluorescent species.^{31, 41} The transfer reaction of the fluorescent ANS species was selectively measured through the PMF measurements, although the voltammetric data were influenced by the adsorption response of the polycationic DGLs. As shown in **Figure 6**, the PMF responses were mainly observed around $\Delta_0^w \phi_{\text{ANS}}^{1/2}$. The PMF signal associated with a quasi-reversible ion transfer (ΔF_t) is correlated with the faradaic ac current ($i_{f,\text{ac}}$). ΔF_t in TIR excitation is described as^{31, 42}

$$\Delta F_t = \frac{4.606\varepsilon\Phi_f I_0}{j\omega zFS \cos\psi} i_{f,\text{ac}} \quad (2)$$

where ε is the molar absorption coefficient, Φ_f is the fluorescence quantum yield, I_0 is the intensity of excitation light, F is Faraday constant, and S is the interfacial area. The real ($\Delta F_{t,\text{re}}$) and imaginary ($\Delta F_{t,\text{im}}$) components of ΔF_t can be expressed by

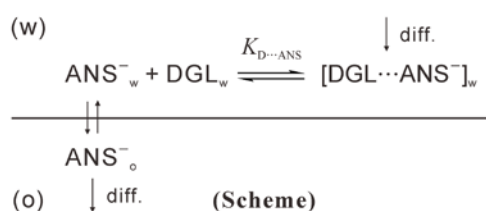
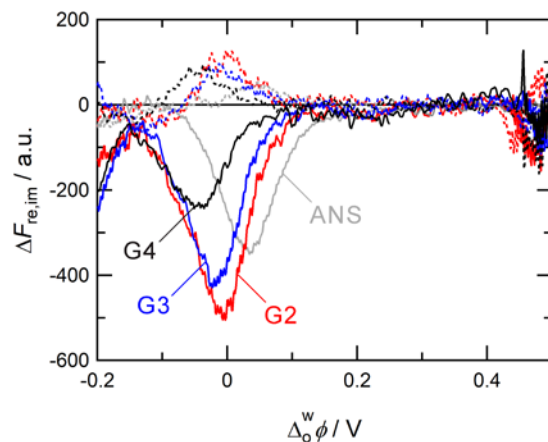


Figure 6. PMF responses measured in the presence of equimolar DGL and ANS and (b) . The black, blue, red, and gray lines depict the DGL-G4-ANS (pH 7.0), G3-ANS (pH 7.1), G2-ANS (pH 7.1), and ANS alone (pH 7.2) systems, respectively. The solid and dashed lines refer to the real (ΔF_{re}) and imaginary (ΔF_{im}) components of PMF signals. The potential sweep rate and the amplitude of ac potential modulation were 0.005 V s^{-1} and 0.020 V at 1 Hz , respectively. The concentration of DGLs and ANS was $1.0 \times 10^{-5} \text{ mol dm}^{-3}$. **(Scheme)** The reaction scheme for the transfer of ANS^- across the interface including the ion association with DGL in the aqueous phase. The subscripts w and o denote the aqueous and organic phases, respectively.

$$\Delta F_{\text{t, re}} = \frac{4.606 \varepsilon \Phi_f I_0}{zFS \cos \psi} \left[\frac{\Delta_0^w \phi_{\text{ac}} \sigma \omega^{-3/2}}{(R_{\text{ct}} + \sigma \omega^{-1/2})^2 + (\sigma \omega^{-1/2})^2} \right] \quad (3)$$

$$\Delta F_{t,im} = -\frac{4.606\varepsilon\Phi_f I_0}{zFS \cos\psi} \left[\frac{\Delta_o^w \phi_{ac} (R_{ct} + \sigma\omega^{-1/2})\omega^{-1}}{(R_{ct} + \sigma\omega^{-1/2})^2 + (\sigma\omega^{-1/2})^2} \right] \quad (4)$$

where R_{ct} is the charge transfer resistance and σ is the Warburg term. Eqs.(3) and (4) provide negative $\Delta F_{t,re}$ and positive $\Delta F_{t,im}$ values for an anionic species, e.g., ANS^- ($z = -1$). The real (ΔF_{re}) and imaginary (ΔF_{im}) components of PMF response with negative and positive signs in **Figure 6** relate basically to the ion transfer of ANS^- across the interface, while the relatively small ΔF_{im} intensities imply a certain contribution from a kinetically controlled adsorption process in the interfacial mechanism.⁴² The PMF responses at $\Delta_o^w \phi > 0.45$ V in the presence of DGLs could arise from the interfacial process of the DGL-ANS associates. The weak PMF signals at the positive edge of the potential window should, however, not be discussed in detail. It is worth noting that the PMF responses around $\Delta_o^w \phi_{ANS}^{1/2}$ were negatively shifted from $\Delta_o^w \phi_{ANS^-}^{o'}$ by adding DGLs in agreement with the voltammetric data (cf. **Figure 5**). The Gibbs free energy of ion association between the DGL and ANS^- ($\Delta G_{D...ANS}$) in aqueous solution can be estimated from the apparent shift of transfer potential.^{26, 27}

$$\Delta_o^w \phi_{ANS}^{1/2} = \Delta_o^w \phi_{ANS^-}^{o'} - \frac{(\Delta G_{D...ANS})_{pH}}{zF} \quad (5)$$

where $\Delta_o^w \phi_{ANS}^{1/2}$ is the half-wave potential for the transfer of ANS determined from the PMF analysis, and z is the charge number of the transferring anion (-1). The $\Delta G_{D...ANS}$ values were analyzed from the PMF data measured at pH 7.0–7.2 in the presence of equimolar DGLs and ANS (1.0×10^{-5} mol dm⁻³) and summarized in **Table 1**. The magnitude of negative $\Delta G_{D...ANS}$ increased gradually with increasing the dendritic generation and the $\Delta G_{D...ANS}$ values indicate the highest stability of the DGL-G4-ANS associate. The association constants between DGL and ANS are

calculated by a simple expression ($\Delta G_{D...ANS} = -RT \ln K_{D...ANS}$) as $\log K_{D...ANS} =$ (DGL-G2) 0.66, (DGL-G3) 0.83, and (DGL-G4) 1.3, respectively. The $\log K_{D...ANS}$ values are considered as the association constant in the aqueous phase assuming no specific interaction from free DGLs weakly adsorbed at $\Delta_0^w \phi_{ANS}^{1/2}$ (**Figure 6(Scheme)**).

Table 1. Gibbs Free Energies of Ion Association between Dendritic Polymers and ANS ($\Delta G_{D...ANS}$) at pH 7 Estimated from the PMF Analysis

	$\Delta_0^w \phi_{ANS}^{1/2} / V$	$\Delta G_{D...ANS} / kJ mol^{-1}$	net charge
DGL-G4 + ANS	-0.048	-7.5±0.4	+366 (+281) ^a
DGL-G3 + ANS	-0.019	-4.7±0.1	+124 (+93) ^a
DGL-G2 + ANS	-0.009	-3.8±0.3	+49 (+42) ^a
G4 PAMAM + ANS	-0.039	-6.9±0.1	+83 ^b
ANS	0.032		

^a Total numbers of free α - and ϵ -amino groups of DGL (number of ϵ -amino groups).⁹

^b Net charge of the PAMAM dendrimer was calculated from pK_a values in literature.³⁵

Assuming a spherical molecular geometry of the G4 PAMAM dendrimer, it has the intermediate characteristics among the dendritic polymers examined in the present study. The net charge and radius of gyration of the PAMAM dendrimer are ca. +83 and 2.2 nm at pH 7.0, respectively.^{35, 43} The PMF responses measured in the presence of equimolar G4 PAMAM dendrimer and ANS exhibit intense signals around 0.4 V (**Figure 7**). The analogous PMF responses have been reported for the PAMAM dendrimer-anionic porphyrin associates.^{22, 27} Those PMF responses result from the transfer of the PAMAM dendrimer binding fluorescent species accompanied by the adsorption at the water|DCE interface. The PMF responses for the ANS transfer at -0.039 V, which were negatively shifted from the intrinsic transfer responses of ANS at 0.032 V, corresponds to the $\Delta G_{D...ANS}$ value of -6.9±0.1 kJ mol⁻¹ (i.e. $\log K_{D...ANS} = 1.2$). In the

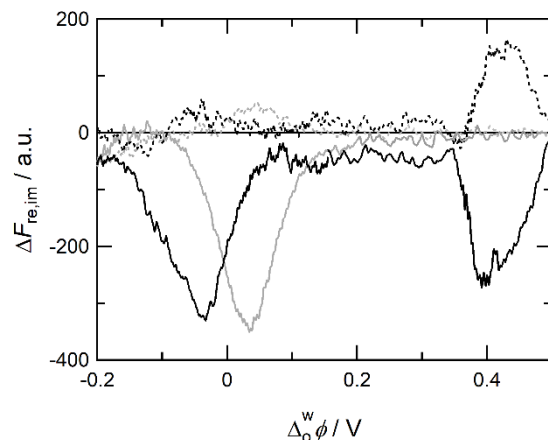


Figure 7. PMF responses measured in the presence of equimolar G4 PAMAM dendrimer and ANS. The black and gray lines depict the G4 PAMAM–ANS (pH 7.0) and ANS alone (pH 7.2) systems, respectively. The solid and dashed lines refer to ΔF_{re} and ΔF_{im} . The potential sweep rate and the amplitude of ac potential modulation were 0.005 V s^{-1} and 0.020 V at 1 Hz , respectively. The concentration of ANS and the dendrimer was $1.0 \times 10^{-5} \text{ mol dm}^{-3}$.

present system, the anionic ANS probe electrostatically binds to cationic sites of the dendritic polymer. Regardless of a smaller net charge of the G4 PAMAM dendrimer than that of DGL-G3, the $\Delta G_{D...ANS}$ values indicate the relatively stable association of ANS^- with the G4 PAMAM dendrimer: $DGL-G4-ANS > G4 \text{ PAMAM-ANS} > DGL-G3-ANS > DGL-G2-ANS$. A recent report by Francoia *et al.* suggested that the polyelectrolyte effect totally prevents the protonation of α -amino groups of DGL at a physiological pH.⁹ Although the α -amino groups of the DGL could be partly protonated under neutral pH conditions, the ϵ -amino groups are mainly responsible for the electrostatic interaction with guest anions. On the other hand, the PAMAM dendrimer has peripheral amino groups and tertiary amines as branch points in the interior. Both cationic sites of the PAMAM dendrimer are capable of associating with anions. In addition, considering the molecular size of the dendritic polymers,^{30, 43} a relatively high charge density of the G4 PAMAM

dendrimer is favorable for interacting with ANS^- . The ion association stability with polycationic dendritic polymers, in general, tends to improve in the case of a multivalent guest molecule. The Gibbs free energy of ion association between the G3.5 PAMAM dendrimer and a bimolecular derivative of ANS, bis- ANS^{2-} , is estimated as -17 kJ mol^{-1} at pH 6.9, while no significant shift of the transfer potential is observed in the monoanionic ANS system.²⁶ Furthermore, the Gibbs free energy of ion association of the G4 PAMAM-tetravalent zinc(II) porphyrin associate has been reported as -30 kJ mol^{-1} . Those multivalent molecules interact with the dendritic polymers via multipoint interaction and entropy effect caused by replacing multiple monovalent counter anions. The ion association stability will be also enhanced for DGL with multivalent guest anions.

4. CONCLUSIONS

The polycationic dendritic polymer, DGL as a potential candidate for molecular carrier in biomedical applications exhibited the anion-binding ability in the wide pH range. The quantitative estimation of the association stability between DGL-G2-G4 and ANS was achieved at the polarized water|DCE interface by the PMF analysis. The $\Delta G_{\text{D}\dots\text{ANS}}$ values obtained from the transfer potential of ANS^- demonstrated that DGL-G4 exerts an efficient stabilizing effect on the ion association, whereas DGL-G2 with less positive charges and small molecular size weakly interacts with ANS. By applying appropriate potentials, the ANS anion was dissociated from its ion associate with DGLs at the interface and transferred into the organic phase, whereas DGLs remained in the aqueous phase. The potential-dependent anion-binding ability of biocompatible DGL under physiological conditions is particularly useful in the development of stimuli-responsive DDS since transmembrane potential changes lead to the drug release process on a cell membrane.

Supporting Information: Emission maximum wavelengths of ANS in the presence of dendritic polymers, excitation and emission spectra measured for DGL-G3 in the presence of phosphate buffers, CVs measured for DGL-G3 at a few supporting electrolyte concentrations, voltammetric data for ANS and the G4 PAMAM dendrimer.

ACKNOWLEDGMENTS

This work was supported by a Grant-in-Aid for Scientific Research (C) (no. 16K05811) from Japan Society for the Promotion of Science (JSPS) and the Kanazawa University CHOZEN Project. The authors are grateful for valuable discussions with Dr. Hiroki Sakae of Okayama University of Science.

REFERENCES

- (1) Kowalczyk, A.; Trzcinska, R.; Trzebicka, B.; Müller, A. H. E.; Dworak, A.; Tsvetanov, C. B., Loading of Polymer Nanocarriers: Factors, Mechanisms and Applications. *Prog. Polym. Sci.* **2014**, *39*, 43-86.
- (2) Fleige, E.; Quadir, M. A.; Haag, R., Stimuli-Responsive Polymeric Nanocarriers for the Controlled Transport of Active Compounds: Concepts and Applications. *Adv. Drug Delivery Rev.* **2012**, *64*, 866-884.
- (3) Ganta, S.; Devalapally, H.; Shahiwala, A.; Amiji, M., A Review of Stimuli-Responsive Nanocarriers for Drug and Gene Delivery. *J. Controlled Release* **2008**, *126*, 187-204.
- (4) Tomalia, D. A., Birth of a New Macromolecular Architecture: Dendrimers as Quantized Building Blocks for Nanoscale Synthetic Polymer Chemistry. *Prog. Polym. Sci.* **2005**, *30*, 294-324.
- (5) Tomalia, D. A.; Christensen, J. B.; Boas, U., *Dendrimers, dendrons, and dendritic polymers: discovery, applications, and the future*. Cambridge University Press: Cambridge, 2012.
- (6) Teertstra, S. J.; Gauthier, M., Dendrigraft polymers: Macromolecular engineering on a mesoscopic scale. *Prog. Polym. Sci.* **2004**, *29*, 277-327.

- (7) Francoia, J.-P.; Vial, L., Everything You Always Wanted to Know about Poly-L-lysine Dendrigrfts (but were afraid to ask). *Chem. Eur. J. in press*, 10.1002/chem.201704147.
- (8) Ibrahim, A.; Koval, D.; Kašička, V.; Faye, C.; Cottet, H., Effective Charge Determination of Dendrigrft Poly-L-lysine by Capillary Isotachophoresis. *Macromolecules* **2013**, *46*, 533-540.
- (9) Francoia, J. P.; Rossi, J. C.; Monard, G.; Vial, L., Digitizing Poly-L-lysine Dendrigrfts: From Experimental Data to Molecular Dynamics Simulations. *J. Chem. Inf. Model.* **2017**, *57*, 2173-2180.
- (10) Tsogas, I.; Theodossiou, T.; Sideratou, Z.; Paleos, C. M.; Collet, H.; Rossi, J. C.; Romestand, B.; Commeyras, A., Interaction and Transport of Poly(L-lysine) Dendrigrfts through Liposomal and Cellular Membranes: The Role of Generation and Surface Functionalization. *Biomacromolecules* **2007**, *8*, 3263-3270.
- (11) Chen, H.; Tian, J.; Liu, D.; He, W.; Guo, Z., Dual Aptamer Modified Dendrigrft Poly-L-lysine Nanoparticles for Overcoming Multi-drug Resistance through Mitochondrial Targeting. *J. Mater. Chem. B* **2017**, *5*, 972-979.
- (12) Kodama, Y.; Nakamura, T.; Kurosaki, T.; Egashira, K.; Mine, T.; Nakagawa, H.; Muro, T.; Kitahara, T.; Higuchi, N.; Sasaki, H., Biodegradable Nanoparticles Composed of Dendrigrft Poly-L-lysine for Gene Delivery. *Eur. J. Pharm. Biopharm.* **2014**, *87*, 472-479.
- (13) Sisavath, N.; Leclercq, L.; Le Saux, T.; Oukacine, F.; Cottet, H., Study of Interactions between Oppositely Charged Dendrigrft Poly-L-lysine and Human Serum Albumin by Continuous Frontal Analysis Capillary Electrophoresis and Fluorescence Spectroscopy. *J. Chromatogr. A* **2013**, *1289*, 127-132.
- (14) Sideratou, Z.; Sterioti, N.; Tsiourvas, D.; Tziveleka, L. A.; Thanassoulas, A.; Nounesis, G.; Paleos, C. M., Arginine End-functionalized Poly(L-lysine) Dendrigrfts for the Stabilization and Controlled Release of Insulin. *J. Colloid Interface Sci.* **2010**, *351*, 433-441.
- (15) Hofman, J.; Buncek, M.; Haluza, R.; Streinz, L.; Ledvina, M.; Cigler, P., In Vitro Transfection Mediated by Dendrigrft Poly(L-lysines): The Effect of Structure and Molecule Size. *Macromol. Biosci.* **2013**, *13*, 167-176.
- (16) Girault, H. H., Electrochemistry at Liquid-Liquid Interfaces. In *Electroanalytical Chemistry*, Bard, A. J.; Zoski, C. G., Eds. CRC Press: 2010; Vol. 23, pp 1-104.

- (17) Senda, M.; Kubota, Y.; Katano, H., Voltammetric study of drugs at liquid-liquid interfaces. In *Liquid interfaces in chemical, biological, and pharmaceutical applications*, Volkov, A. G., Ed. Marcel Dekker: New York, 2001; pp 683-698.
- (18) Kontturi, K.; Murtomaki, L., Electrochemical Determination of Partition-Coefficients of Drugs. *J. Pharm. Sci.* **1992**, *81*, 970-975.
- (19) Reymond, F.; Chopineaux-Courtois, V.; Steyaert, G.; Bouchard, G.; Carrupt, P. A.; Testa, B.; Girault, H. H., Ionic Partition Diagrams of Ionisable Drugs: pH-Lipophilicity Profiles, Transfer Mechanisms and Charge Effects on Solvation. *J. Electroanal. Chem.* **1999**, *462*, 235-250.
- (20) Deryabina, M. A.; Hansen, S. H.; Jensen, H., Molecular Interactions in Lipophilic Environments Studied by Electrochemistry at Interfaces between Immiscible Electrolyte Solutions. *Anal. Chem.* **2008**, *80*, 203-208.
- (21) Nakamura, M.; Osakai, T., Evaluation of the Membrane Permeability of Drugs by Ion-Transfer Voltammetry with the Oil|Water Interface. *J. Electroanal. Chem.* **2016**, *779*, 55-60.
- (22) Nagatani, H.; Ueno, T.; Sagara, T., Spectroelectrochemical Analysis of Ion-Transfer and Adsorption of the PAMAM Dendrimer at a Polarized Liquid|Liquid Interface. *Electrochim. Acta* **2008**, *53*, 6428-6433.
- (23) Nagatani, H.; Sakae, H.; Torikai, T.; Sagara, T.; Imura, H., Photoinduced Electron Transfer of PAMAM Dendrimer-Zinc(II) Porphyrin Associates at Polarized Liquid|Liquid Interfaces. *Langmuir* **2015**, *31*, 6237-6244.
- (24) Sakae, H.; Fujisawa, M.; Nagatani, H.; Imura, H., Molecular Association between Flavin Derivatives and Dendritic Polymers at the Water|1,2-Dichloroethane Interface. *J. Electroanal. Chem.* **2016**, *782*, 288-292.
- (25) Sakae, H.; Nagatani, H.; Imura, H., Ion Transfer and Adsorption Behavior of Ionizable Drugs Affected by PAMAM Dendrimers at the Water|1,2-Dichloroethane Interface. *Electrochim. Acta* **2016**, *191*, 631-639.
- (26) Nagatani, H.; Sakamoto, T.; Torikai, T.; Sagara, T., Encapsulation of Anilino-naphthalenesulfonates in Carboxylate-Terminated PAMAM Dendrimer at the Polarized Water|1,2-Dichloroethane Interface. *Langmuir* **2010**, *26*, 17686-17694.
- (27) Sakae, H.; Nagatani, H.; Morita, K.; Imura, H., Spectroelectrochemical Characterization of Dendrimer-Porphyrin Associates at Polarized Liquid|Liquid Interfaces. *Langmuir* **2014**, *30*, 937-945.

- (28) Herzog, G.; Flynn, S.; Arrigan, D. W. M., Macromolecular Sensing at the Liquid-Liquid Interface. *J. Phys.: Conf. Ser.* **2011**, *307*, 012055.
- (29) Herzog, G.; Flynn, S.; Johnson, C.; Arrigan, D. W. M., Electroanalytical Behavior of Poly-L-Lysine Dendrigrafts at the Interface between Two Immiscible Electrolyte Solutions. *Anal. Chem.* **2012**, *84*, 5693-5699.
- (30) Cottet, H.; Martin, M.; Papillaud, A.; Souaïd, E.; Collet, H.; Commeyras, A., Determination of Dendrigraft Poly-L-Lysine Diffusion Coefficients by Taylor Dispersion Analysis. *Biomacromolecules* **2007**, *8*, 3235-3243.
- (31) Nagatani, H.; Sagara, T., Potential-Modulation Spectroscopy at Solid/Liquid and Liquid/Liquid Interfaces. *Anal. Sci.* **2007**, *23*, 1041-1048.
- (32) Wandlowski, T.; Mareček, V.; Samec, Z., Galvani Potential Scales for Water-Nitrobenzene and Water-1,2-Dichloroethane Interfaces. *Electrochim. Acta* **1990**, *35*, 1173-1175.
- (33) Hawe, A.; Sutter, M.; Jiskoot, W., Extrinsic Fluorescent Dyes as Tools for Protein Characterization. *Pharm. Res.* **2008**, *25*, 1487-1499.
- (34) Slavík, J., Anilinothalene Sulfonate as a Probe of Membrane Composition and Function. *Biochim. Biophys. Acta, Rev. Biomembr.* **1982**, *694*, 1-25.
- (35) Leisner, D.; Imae, T., Polyelectrolyte Behavior of an Interpolyelectrolyte Complex Formed in Aqueous Solution of a Charged Dendrimer and Sodium Poly(L-glutamate). *J. Phys. Chem. B* **2003**, *107*, 13158-13167.
- (36) Cakara, D.; Kleimann, J.; Borkovec, M., Microscopic Protonation Equilibria of Poly(amidoamine) Dendrimers from Macroscopic Titrations. *Macromolecules* **2003**, *36*, 4201-4207.
- (37) Shcharbin, D.; Szwedzka, M.; Bryszewska, M., Does Fluorescence of ANS Reflect Its Binding to PAMAM Dendrimer? *Bioorg. Chem.* **2007**, *35*, 170-174.
- (38) Jin, X.; Leclercq, L.; Sisavath, N.; Cottet, H., Investigating the Influence of Phosphate Ions on Poly(L-lysine) Conformations by Taylor Dispersion Analysis. *Macromolecules* **2014**, *47*, 5320-5327.
- (39) Stuart, M. A. C.; Huck, W. T. S.; Genzer, J.; Müller, M.; Ober, C.; Stamm, M.; Sukhorukov, G. B.; Szleifer, I.; Tsukruk, V. V.; Urban, M.; Winnik, F.; Zauscher, S.; Luzinov, I.; Minko, S., Emerging Applications of Stimuli-responsive Polymer Materials. *Nat. Mater.* **2010**, *9*, 101-113.

- (40) Berduque, A.; Scanlon, M. D.; Collins, C. J.; Arrigan, D. W. M., Electrochemistry of Non-Redox-Active Poly(propylenimine) and Poly(amidoamine) Dendrimers at Liquid–Liquid Interfaces. *Langmuir* **2007**, *23*, 7356-7364.
- (41) Nagatani, H., *In Situ* Spectroscopic Characterization of Porphyrins at Liquid Interfaces. In *Handbook of Porphyrin Science*, Kadish, K. M.; Smith, K. M.; Guillard, R., Eds. World Scientific Publishing Co.: Singapore, 2014; Vol. Volume 34: Harnessing Solar Energy pp 51-96.
- (42) Nagatani, H.; Fermín, D. J.; Girault, H. H., A Kinetic Model for Adsorption and Transfer of Ionic Species at Polarized LiquidjLiquid Interfaces as Studied by Potential Modulated Fluorescence Spectroscopy. *J. Phys. Chem. B* **2001**, *105*, 9463-9473.
- (43) Maiti, P. K.; Cagin, T.; Lin, S. T.; Goddard III, W. A., Effect of Solvent and pH on the Structure of PAMAM Dendrimers. *Macromolecules* **2005**, *38*, 979-991.

TOC GRAPHICS

